5th International Conference on Civil Engineering, Architecture and Urban Planning Elites
Paris, France November 2-4, 2018

Energy Evolution and Blast Response of Segmented Circular Tunnels; Considering Depth and Different Soils

Zia Hoseini *

*School of civil engineering, Damghan University, P.O.Box 36715-364, Damghan Iran.

Abstract

Energy assessment of deep tunnels depends on the depth and what kind of ground they surrounded by .The numerical results showed that high static compressive stress concentration around the underground tunnel results in the accumulation of substantial strain energy at the same location. The roof and floor of the tunnel are more prone to dynamic failures during the blasting loading process. the analysis of energy dissipation indicated that the strain energy reduction and the residual kinetic energy are positively related to the lateral pressure coefficient and the burial depth of the tunnel, and the residual kinetic energy is much larger than the strain energy reduction under the same condition. Furthermore, for an underground tunnel subjected to high in situ stress, the blasting stress wave with lower amplitude is sufficient to trigger severe dynamic failures. Results indicate that a tunnel in saturated soil is more vulnerable to severe damage than that buried in either partially saturated soil or dry soil. The tunnel is also more vulnerable to surface explosions that occur directly above the centre of the tunnel than those that occur at any equivalent distance in the ground away from the tunnel centre.

Keywords: Dynamic stress concentration, Energy evolution, Blasting load, Numerical simulation, soil

1. INTRODUCTION

In recent years, the exhaustion of mineral resources in shallow depths, and the rapid development of tunneling and hydropower engineering, have considerably motivated the tunnel excavations to extend to depth. However, due to the complicated geological environment in which deep excavations are carried out, a large number of unconventional rock failure phenomena such as spalling,[1], [2] zonal disintegration phenomenon [3], [4] and rock burst hazards [5],[6] have been observed during underground excavations. These accidents or hazards will bring about damages to equipment and delays of excavation operation, and even pose great threats to the safety of construction personnel. Therefore, it is an urgent issue to figure out the mechanism of the engineering disasters occurring in deep excavations. In practice, underground rocks and ores are naturally stressed by gravitational and tectonic stress. When an underground tunnel is excavated, the previous stress states existing in rock mass are disturbed, with the radial principal stress being released and tangential principal stress concentrating in the periphery of the tunnel.[7][8][9] in this process, the strain energy releases at some locations while accumulating at other locations, which leads to different mechanical responses of underground tunnels under dynamic disturbance.[10][11] In addition, during the underground excavation process, the excavation damaged zone (EDZ) is formed in the proximity of the excavated tunnel. To date, considerable research efforts were devoted to investigating the formation of EDZ and the fracture mechanisms of surrounding rock during underground excavations. [12][13][14][15][16][17] For instance, a series of studies have been carried out at the Underground Research Laboratory (URL) since 1983 to study excavation responses when underground openings were excavated.[13][14] Findings of these works showed that various factors such as the nearfield stress history, geological variability, excavation method, tunnel geometry, and confining pressure are responsible for the excavation damage and instability of underground openings. The presence of the EDZ around an underground opening in turn has a great influence on the mechanical, hydraulic, and thermal characteristics of surrounding rock masses, few reports have considered the effect of dynamic disturbance. Many evidences showed that, during underground excavations, dynamic disturbance such as explosion-induced vibrations from adjacent tunnel and stress impact from neighboring rock bursts have a significant influence on existing tunnels.[18][19][20] Therefore, the dynamic disturbance is an important factor to be considered when studying the stability of deep-buried tunnel.

The drill and blast (D&B) method is extensively used in mining and tunneling engineering, because it is still an economical and efficient excavation approach for rock fracture and fragmentation.[21] When the drill and blast method is used in underground excavations, the blasting vibration is generated and propagates to the deep of surrounding rock mass in the form of stress waves, which may cause damage to not only the surrounding rock mass but also nearby structures.[22][23] Therefore, many researchers have conducted a lot of studies on the dynamic responses of structures subjected to blast-induced stress waves, aiming at putting forward more reasonable and effective support schemes. For instance, Malmgren and Nordlund[24] analyzed the dynamic behaviors of shotcrete supported rock wedges subjected to blast-induced vibrations based on field measurement data in the Pabedana(Kerman ,Iran) coal mine, and indicated that a wedge can be ejected by a dynamic load even if the static safety factor is larger than 10. Therefore, the support system was suggested to be able to consume energy in order to support the rock wedges subjected to blasting loads.

Based on the modeling results, the authors proposed a new approach for tunnel support designs to withstand spalling induced by blasting loads. With rapid development of computer technology, numerical simulation techniques have become economical and powerful tools for modeling rock mechanics and rock engineering.[28][29] Using numerical analysis methods, many researchers have carried out various studies on the dynamic response of rock mass and underground structures under dynamic disturbance. The boundary element method (BEM) was used by Stamos and Beskos[30] to determine the dynamic response of large three-dimensional underground structures subjected to dynamic loads or seismic waves. Wang et al.[31] analyzed dynamic fracture behaviors of rock in tension due to blast loading using a finite element method (FEM) code LS-DYNA. Ning et al.[32][33] implemented the discontinuous deformation analysis (DDA) to simulate the rock mass failures by the blast-induced high pressure expansion. In their numerical model, the whole process of the blast chamber expansion, explosion gas penetration, rock mass failure and cast, and the formation of the final blasting pile can be wholly reproduced. In addition, the finite difference method (FDM) based program FLAC3D was used by Wang et al.[34] to study the dynamic response of underground gas storage salt cavern under seismic loads. As for dynamic responses of underground tunnels under dynamic disturbance, Zhu et al.[35]. This paper provides an insight into the mechanism of rockbursts in the periphery of underground tunnels, as well as guidance for the design in support of depth and different surrounding soils.

The four key factors that affect the tunnel response under blast loading are: (a) surrounding ground type, (b) explosive mass, (c) standoff distance and (d) lining stiffness. Although the lining stiffness is the engineer’s choice, it may be difficult to evaluate how the tunnel response is influenced by its stiffness. The response of the segmented tunnel lining to the blast loading is more complex than that to other loadings such as geostatic and earthquake loadings. However, there is inadequate information on the response of bored tunnels to blast loading. It is therefore of interest to investigate the vulnerability of segmented tunnels to credible blast loading.

2. Theoretical formulation of the dynamic response of a circular tunnel

In theoretical analysis, it is assumed that a circular tunnel is excavated along the direction parallel to the principal stress, so the problem can be approximately regarded as a plane strain case. For an underground tunnel subjected to dynamic stress waves, according to the superposition principle,[44] the stress, displacement and velocity components of the rock or soil mass around the tunnel can be obtained by superimposing the static component induced by in situ stress with the dynamic component induced by incident plane wave under unstressed condition. However, due to the stress and deformation induced by in situ stress are time-independent, the dynamic stress wave is only considered when theoretically investigating the dynamic response of underground tunnel. In the view of wave mechanics, the problem of the interactions between stress wave and underground opening can be regard as the initial-boundary value problem of wave equation. In this section, we focus on the dynamic responses of underground tunnel subjected to blasting load, which can be simplified as an analysis of circular hole subjected to a plane P wave as shown in Fig. 1, where x and y are the Cartesian coordinate system, θ and r are the Polar coordinate system, and a is the radius of tunnel. As the transient response induced by any form of transient loading can be determined by superposing harmonic waves of all frequencies, it is necessary to first determine a theoretical formulation under harmonic wave excitation, which was described in detail by Mow and Pao.[45].

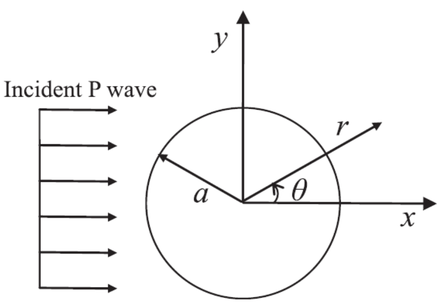

Fig. 1. Simplified model of interactions between incident P wave and underground tunnel.

As shown in Fig. 1, a harmonically time-varying incident plane P wave propagates along the positive direction of axis x, and the incident wave can be expressed as:

$$\varphi^{(i)} = \varphi_0 e^{i(\alpha x - \omega t)} \qquad \textbf{(Eq.1)}$$

where α=ω/cp is the P wave number, ϕ0 is the amplitude, ω is the circular frequency, and cp is the P wave velocity.

In terms of the wave function expansion method, the incident wave function can be expanded as:

$$\varphi^{(i)} = \varphi_0 \sum_{n=0}^{\infty} \varepsilon_n i^n J_n(\alpha r)\cos(n\theta)e^{-i\omega t} \qquad \textbf{(Eq.2)}$$

When an incident plane P-wave propagates through a circular hole, a compressional wave (P wave) and a shear wave (SV wave) arise from the circular hole boundary, because the reflecting surface is not perpendicular to the direction of P wave incidence. The SH wave is not generated because it causes rock particles to oscillate perpendicular to the analyzed plane.44 P and SV waves can be expressed as:

$$\varphi^{(r)} = \sum_{n=0}^{\infty} A_n H_n^{(1)}(\alpha r)\cos(n\theta)e^{-i\omega t} \qquad \textbf{(Eq.3)}$$

$$\psi^{(r)} = \sum_{n=0}^{\infty} B_n H_n^{(1)}(\beta r)\sin(n\theta)e^{-i\omega t} \qquad \textbf{(Eq.4)}$$

where *φ*(*r*) and *ψ*(*r*) are the reflected P wave and the reflected S wave, respectively, which represent waves diverging from the origin, β=ω/cs is the S wave number, cs is the S wave velocity, *Hn* (*x*) (1) is the first type of Hankel function, An and Bn are coefficients of the expressions that can be determined from the appropriate boundary conditions.

$$\overline{\sigma}_{\theta\theta}|_{r=a} = \frac{\sigma_{\theta\theta}}{\sigma_0} = \frac{4}{\pi}\left(1 - \frac{1}{\kappa^2}\right)\sum_{n=0}^{\infty} \varepsilon_n i^{n+1} s_n \cos(n\theta) e^{-i\omega t} \qquad \textbf{(Eq.5)}$$

When $t_r \leq t < t_s$, we have:

$$\begin{aligned} g(x_i, t) &= \int_0^{t_r} \frac{1}{t_r} d\tau \frac{2}{\pi} \int_0^{\infty} \frac{R(\omega)\sin\omega(t-\tau)}{\omega} d\omega \\ &+ \int_{t_r}^{t} \frac{-1}{t_s - t_r} d\tau \frac{2}{\pi} \int_0^{\infty} \frac{R(\omega)\sin\omega(t-\tau)}{\omega} d\omega \\ &= \frac{2}{\pi t_r} \int_0^{\infty} \frac{R(\omega)[\cos\omega(t-t_r) - \cos\omega t]}{\omega^2} d\omega \\ &- \frac{2}{\pi(t_s - t_r)} \int_0^{\infty} \frac{R(\omega)[1 - \cos\omega(t-t_r)]}{\omega^2} d\omega \end{aligned} \qquad \textbf{(Eq.6)}$$

Now we can determine the transient stress behaviors of the tunnel under blasting load using Eq. (6). However, it is also cumbersome to take a direct integration of Eq. (6) due to the difficulties associated with obtaining analytical expression of R(ω). In this paper, R(ω) is precisely the real part of Eq. (5), which can be obtained by determining the relationship between $\sigma\vartheta\vartheta$ and all wave numbers using Eq. (5). Once we have the numerical results of R(ω) with all wave numbers, we can substitute them with a sum of trapezoid functions. In turn, the sum of the simple responses can yield the total dynamic responses.[47] This approach has proved to be an effective way to determine dynamic responses of tunnel subjected to transient loads.[44][48] The numerical integration mentioned above can be calculated by a MATLAB code.

3.Numerical results and analysis

In this section, the physical properties of the rock specimen extracted from the Kaiyang Phosphate Mine were employed to calculate the dynamic responses mentioned above. The density, Yong's modulus and Poisson's ratio of the rock specimen are 2750 kg/m3, 18.73 GPa and 0.206, respectively. The numerical results of the dynamic stress concentration factor (DSCF) variations at the tunnel boundary are presented in Fig. 2, where τr is the normalized rising time of the blasting load, and ts/tr is the ratio of the total time to the rising time, which characterizes the unloading speed during blasting load. The smaller the ts/tr ratio is, the faster the unloading speed it means. When ts/tr =1, it means instantaneous unloading of blasting load. As the dynamic responses are related to the observation locations and loading parameters, DSCF variations at θ= 0, π/2 and π with ts/tr =5 and 10 are shown in Fig. 2.

Numerical results in Fig. 2 indicate that obvious dynamic stress concentration generated at tunnel boundary during blasting loading process, which is characterized by compressive stress concentration at θ=π/2 and tensile stress concentration at θ=0 and π. The DSCF at θ=π/2 is much larger than that at θ=0 and π. The DSCF time-history curves at θ=0 and π have approximately the same shapes. In loading process, DSCF increases rapidly to the first positive peak value and then declines to the minimum value; in unloading process, DSCF increases from the minimum value to the secondary positive peak value and then decreases to zero. While the DSCF curves at θ=π/2 have different shapes, only one positive peak value and one negative peak value appear during loading and unloading process.

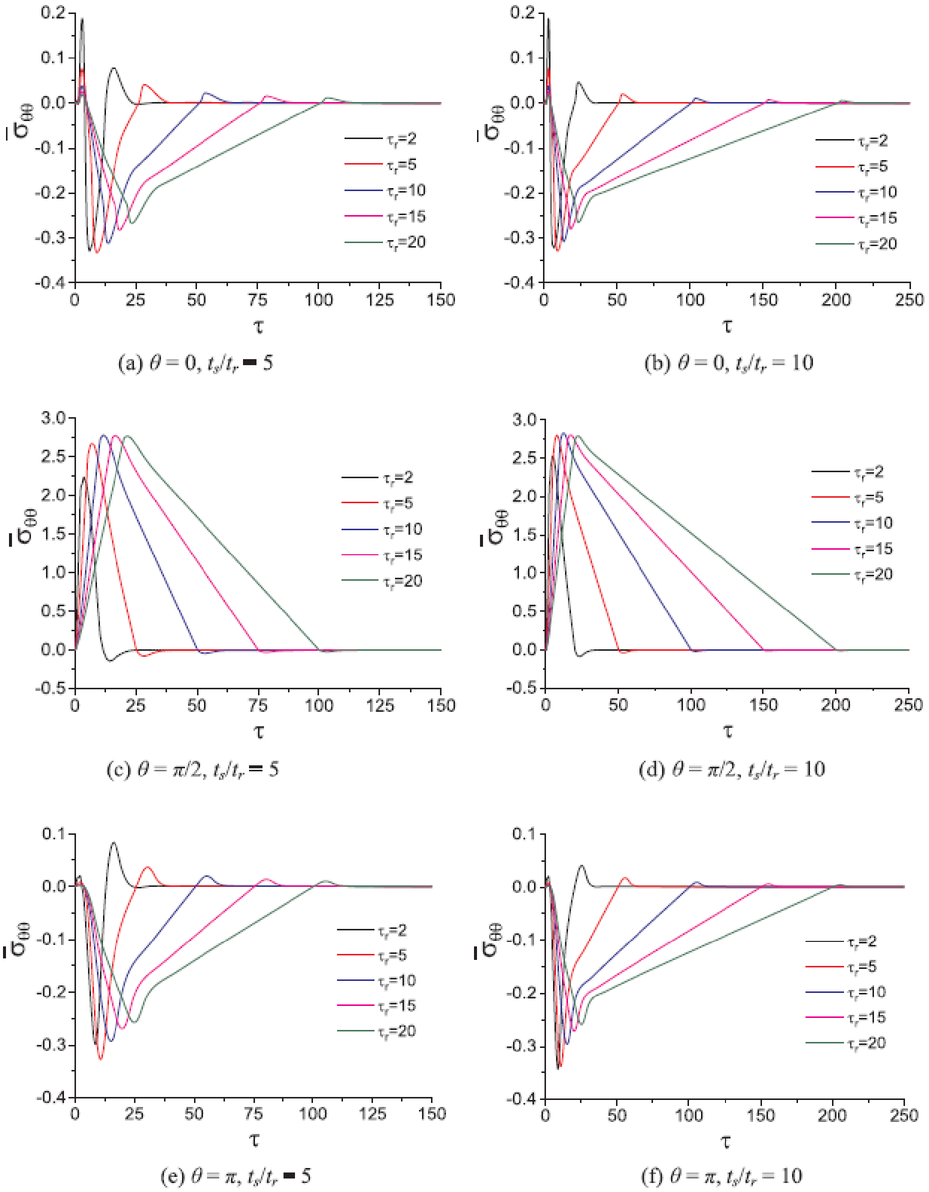

Fig. 2. Numerical results of the DSCF at tunnel boundary.

In the entire processes, the loading effect can be represented by the minimum value at θ=0 and π and maximum value at θ=π/2, and the unloading effect can be represented by the secondary positive peak value at θ=0 and π and negative peak value at θ=π/2. It is found that the unloading effect is more dramatic when ts/tr =5 than that when ts/tr =10. For the same ts/tr ratio, the shorter the τr is, the more dramatic unloading effect is. It indicates that shorter duration of blasting load induces more obvious unloading effect. When the duration of blasting load increases to τs

=200, the unloading effect becomes virtually unnoticeable. With the increase of τr, the loading effect converges to the static stress concentration factor, which is given by:[45]

$$\sigma^{*}_{\theta\theta} = \frac{2}{\kappa^2}[(\kappa^2 - 1) - 2\cos 2\theta] \qquad \textbf{(Eq.7)}$$

where κ is the ratio of P to S wave velocity. Eq. (33) is the limit of Eq. (19) when $\alpha \to 0$, which is equivalent to the static solution for biaxial loadings. The static stress concentration factor is 2.74 at θ=π/2 and −0.22 at θ= 0 and π.

3.Dynamic responses of underground tunnel induced by blasting load

In this section, a series of waveforms of blasting load with different rising time (i.e., tr =1 ms, 2 ms, 3 ms, 4 ms and 5 ms) and a constant ts/ tr ratio of 5 were applied to investigate the dynamic responses of the tunnel subjected to coupled static-dynamic loading, the corresponding durations of blasting load are 5 ms, 10 ms, 15 ms, 20 ms and 25 ms. The peak value of blasting load is 15 MPa, and the vertical and horizontal in situ stress is 10 MPa. The numerical simulation results are shown in Fig. 3.

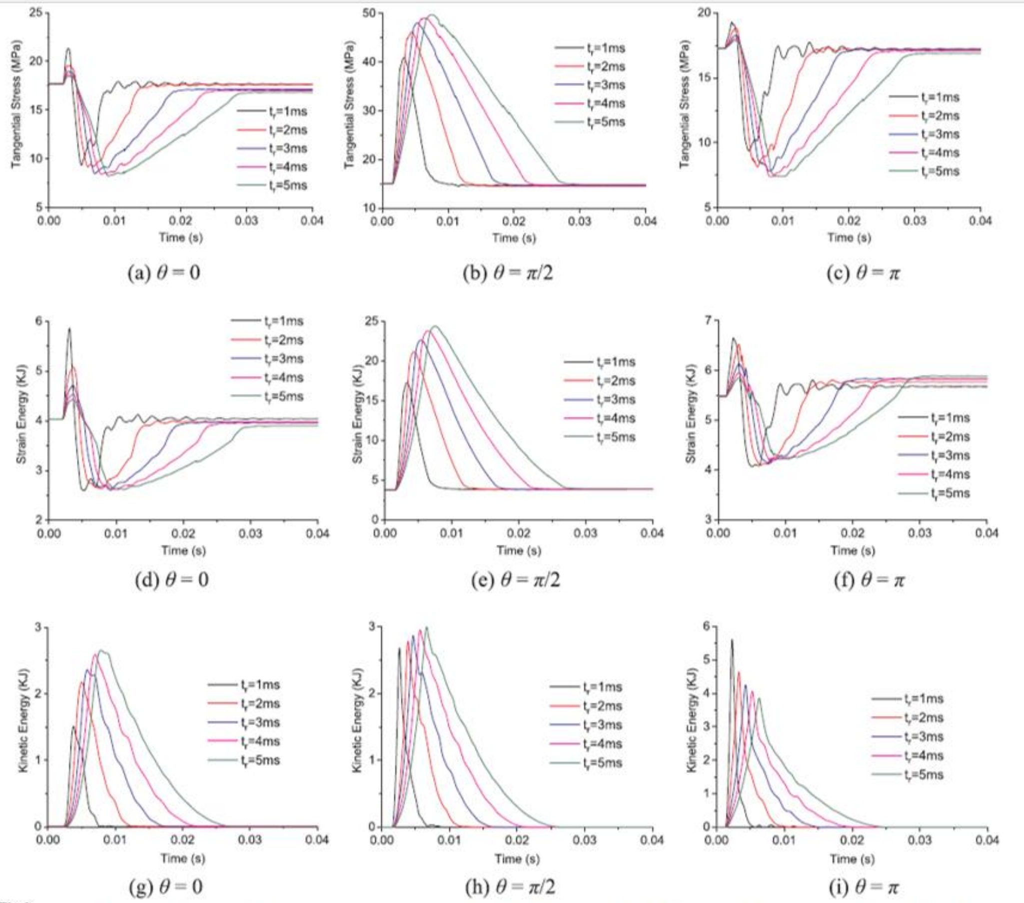

Fig.3 Stress and energy evolutional curves at different monitoring points under various waveforms of blasting load ((a)、(b)、(c): tangential stress evolution, (d)、(e)、(f): strain energy evolution, (g)、(h)、(i): kinetic energy evolution).

Fig. 3a-c presents the tangential stress evolutional curves in different monitoring points at tunnel boundary during dynamic loading, and the positive value indicates the compressive stress. Time begins when dynamic loading was applied to the model boundary. Before dynamic stress wave arrives at tunnel boundary, stress at tunnel boundary remains constant. At t=1.33 ms, dynamic stress wave arrives at the left sidewall of the tunnel, tangential stress at θ=π increases immediately, and then the incident compressive stress wave leads to a reduction of tangential stress at the left sidewall of the tunnel as shown in Fig. 3c. The greater the rising time of blasting load is, the larger the extent of reduction is, but when tr exceeds 4 ms, the extent of reduction hardly increases. Because of the existence of compressive stress induced by static stress, the reduction of tangential stress does not give rise to tensile stress at left sidewall. After the dynamic stress wave passes through, tangential stress at the left sidewall returns to initial value. When t=1.67 ms, dynamic stress wave arrives at the roof and floor of the tunnel, tangential stress at θ=π/2 increases rapidly as shown in Fig. 3b, and a larger rising time of blasting load brings about a higher peak value of tangential stress. When t=2 ms, dynamic stress wave arrives at the right sidewall of the tunnel. As shown in Fig. 3a, the tangential stress evolutional curves at θ= 0 are approximately the same as the curves at θ=π. It can be found from the comparisons between Fig. 3a-c and Fig. 2 that the numerical results are generally consistent with the theoretical results, i.e. under blasting stress wave incidence, the compressive stress at θ=π/2 is much larger than that at θ= 0 and π. However, there are also some differences between theoretical and numerical results, because the theoretical solutions are based on electrodynamics, in which the rock mass is considered as homogeneous, isotropic and perfectly elastic medium, while the numerical model composes of a large number of discrete particles. Besides, the average stress in a measurement circle cannot completely represent the stress on tunnel surface. Fig. 3d-f presents the strain energy evolutional curves in different monitoring points at tunnel boundary during dynamic loading. Comparing Fig. 3a-c with Fig.3d-f, it can be found that the strain energy evolutional curves are similar to the tangential stress evolutional curves at the same monitoring location. It denotes that the accumulation of strain energy around tunnel boundary is the result of the stress redistribution during dynamic loading. The maximum values of strain energy at θ= 0 and π are 5.85 kJ and 6.65 kJ respectively, while it is 24.35 kJ at θ=π/2. The maximum value of strain energy at θ=π/2 is considerably larger than that at θ=0 and π, and the greater the tr is, the larger the value of the maximum strain energy is. It indicates that a dynamic stress wave with high rising time induces a large amount of strain energy accumulating at the roof and floor of the tunnel. Fig. 3g-i presents the kinetic energy evolutional curves in different monitoring points at tunnel boundary during dynamic loading. When dynamic stress wave arrives at the left sidewall of the tunnel, the kinetic energy at θ=π increases rapidly to a peak value as shown in Fig. 3i, the peak value of kinetic energy decreases with the increase of tr, and the maximum kinetic energy is 5.62 kJ when tr =1 ms. It can be observed from Fig. 3g and h that the peak value of kinetic energy at θ= 0 and π/2 increases with the increase of tr, and the maximum values of kinetic energy at θ= 0 and π/2 are 2.66 kJ and 2.99 kJ when tr =5 ms, which are smaller than that at θ=π.

4. Blast Response of Segmented Tunnels in Different Soils

In bored tunnel construction, the soil types can vary along the length of the tunnel. This section investigates the blast response of a segmented tunnel buried in different soil types. Three types of soils that were considered in [34] to investigate the blast effect on buried piles were used in this study.

There are three soil types: saturated soil, partially saturated soil and dry soil. As [34], a similar free-field study was first conducted. The free-field peak pressure attenuation responses for these three soils were consistent with the plots presented in [34]. *Fig.4* shows a comparison of the peak pressure attenuations for the three types of soils as a function of scaled distances. It shows that both the soil type and the degree of water saturation play a large role in determining the peak pressures. The comparison shows that higher peak pressures occur in the saturated clay soil.

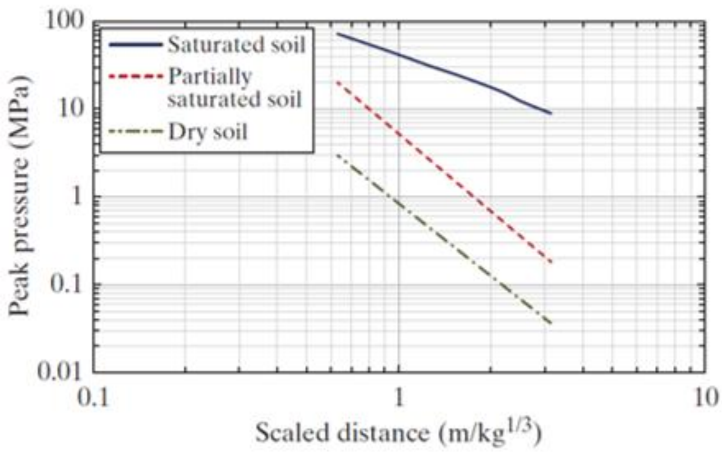

Fig.4 *Comparison of free-field peak pressures*

As described in *Fig. 5*, a common single tube railway tunnel system [30] was considered, having a 150 mm thickness annulus concrete grout of concrete grade 15 around the tunnel. The inner diameter and the thickness of the tunnel lining were 5.8 m and 275 mm, respectively. The segment was 1.4 m in length in the longitudinal direction. As illustrated, the segments were rotated from ring to ring by a 22.5° angle to the tunnel centreline (CL). Both radial and circumferential joints were flat; the reinforcement details are described in *Fig. 5*.

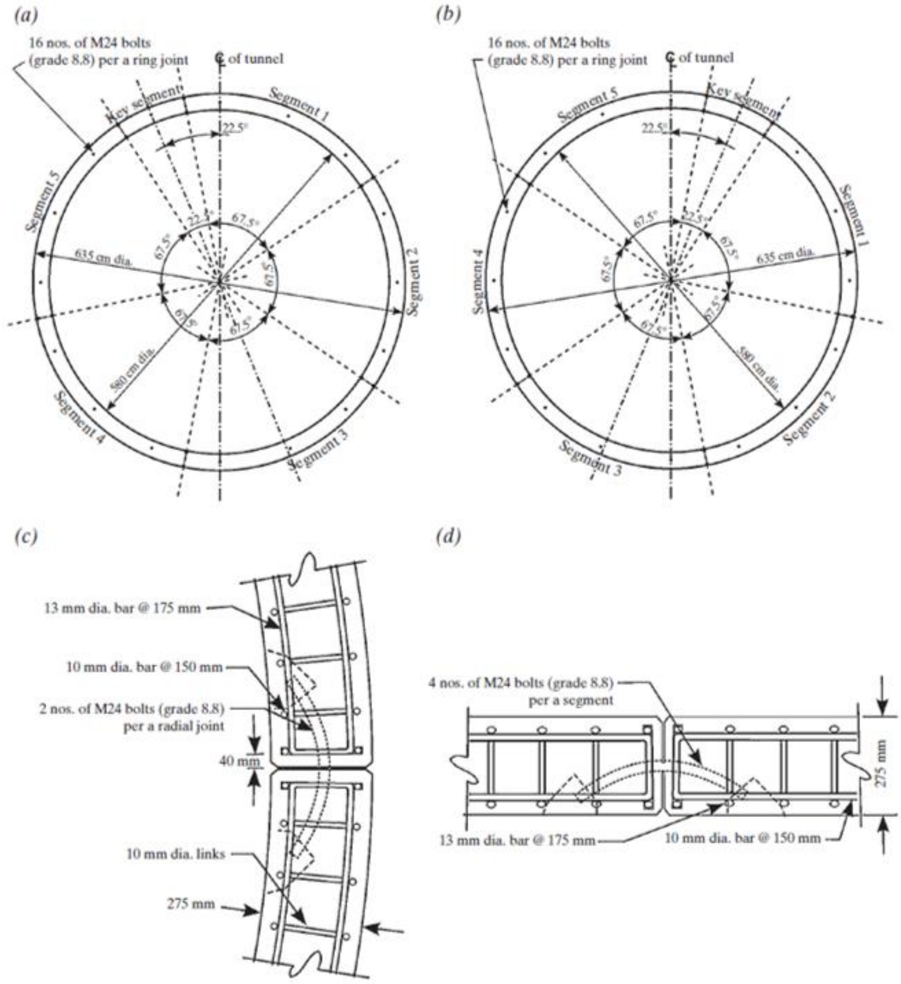

Fig.5 *General arrangement of segments. (a) Key segment: left-hand CL; (b) key segment: right-hand CL; (c) radial joint; and (d) circumferential joint*

Figure 6 represents the three-dimensional numerical model to study the effects of surface blast loading on tunnel response under the influence of the soil properties. Considering the symmetries, half of the structure about ZX plane was modelled with a cylindrical explosive at the ground surface. Grouting of annular gap was achieved by a full round embedment with the surrounding soil. The interface between the grout and the soil was modelled using merged nodes.

However, the interface between the segments and the grout was modelled using the penalty-based surface–surface type contact. Apart from the geometrical aspects of the segments, modelling of the segments and their reinforcements was similar to the modelling of the test slab and the reaction structure.18 The soil properties were changed to investigate their effects on the different aspects of the tunnel response.

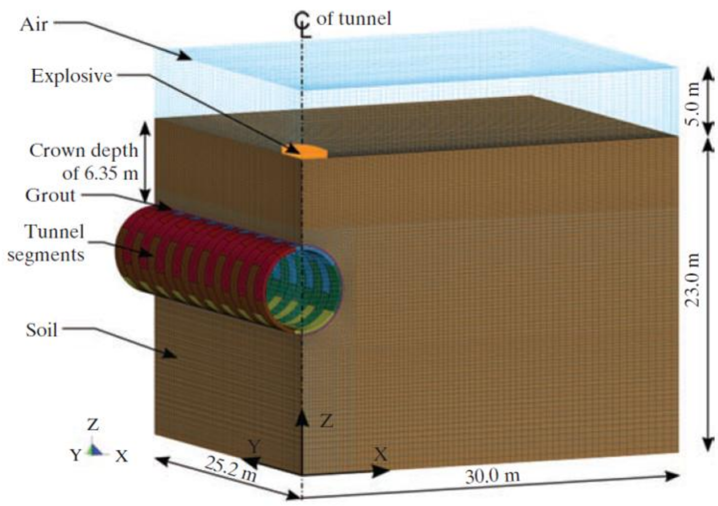

Fig.6 *A half-symmetrical numerical model*

5. The Effect of Tunnel Depth and Stand-off Distance in Blast Impact

There are numerous empirical relationships between the stand-off distance and blast effects due to various explosive weights for free-field explosions. However, the relationship between the stand-off distance and the segmented tunnel response due to a surface blast are not reported. There is no established guideline for predicting either the tunnel response or the characteristics of the blast loading. In this section, the effects of tunnel depth, ground distance and explosive weight on the tunnel response in the saturated soil are studied.

Figure 11a shows that the tunnel depth varied from 6.35 m (1D) to 12.70 m (2D), and the ground distance varied from the tunnel centerline to 12.70 m (2D) as shown in *Fig.7*. Cracks in segments, bolt failure and drifting response were considered as critical factors to evaluate the blast performance of the tunnel structure in this study. The damage states of tunnels can be divided into the following four groups:

1. no damage: the tunnel is considered to behave elastically with some minor cracks in segments (maximum crack width < 0.3 mm31) and no bolt failure;
2. slight damage: a small number of cracks exceed the crack limiting value of 0.3 mm and a few bolts fail at the joints, but the drifting response is insignifi cant;
3. moderate damage: a large number of cracks exceed the crack limiting value of 0.3 mm, a large number of failed bolts trigger signifi cant drifting or sliding of segments at joints; however, the tunnel remains functional by keeping the in-plane tunnel profi le because of hoop compression;

4. severe damage or collapse: formation of full depth cracks, and a large number of bolt failures, resulting in a large drift between segments.

The damage state increases with the intensity of the shock wave impacting the tunnel. Low-energy blast impacts cause little or no damage in the tunnel lining while high-energy blast impacts cause moderate to severe damage.

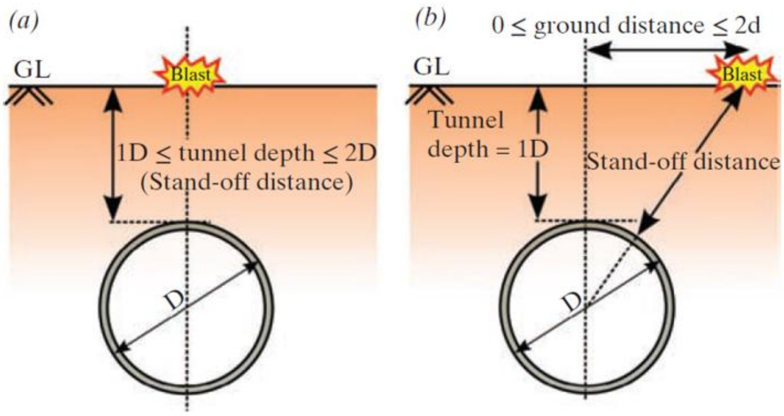

Fig.7 *Variation of tunnel depth and ground distance. (a) Variation of tunnel depth and (b) variation of ground distance (Units: [–])*

6. Conclusion

In this paper, a two-dimensional mathematical physics model was first presented to investigate the dynamic response around a circular tunnel subjected to blasting stress wave excitation. Based on the steady state solution of the wave expansion approach, transient solutions subjected to different incident waveforms were obtained. Theoretical results indicated that the DSCF at the roof and floor of the tunnel is much larger than that at two sidewalls when blasting stress wave was applied to left model boundary, but the dynamic amplification factor at two sidewalls is much larger than that at the roof and floor. The numerical results indicated that, for an underground tunnel only subjected to in situ stress, high compressive stress concentration around the tunnel leads to the accumulation of massive strain energy at the same location. During dynamic loading process, the roof and floor of the tunnel are more vulnerable to dynamic failures. altought, the effect of the dynamic blasting stress wave induced by adjacent tunnel excavations should be taken into consideration when the support and reinforcement systems of an underground tunnel are designed, especially for the tunnel subjected to high in situ stress. Three types of soils were considered first by varying the weight of the explosive on the ground surface, followed by a study to predict the blast response of the segmented tunnel to different scale distances by varying the tunnel depth as well as the ground distance of the explosive from the tunnel centreline.

The main findings of this study are as follows:

− Both soil composition and degree of water saturation have a great impact on the peak pressure response in the soil as well as on the tunnel structure.

− The blast response of a tunnel buried in saturated soil is more severe in terms of crack formation and bolt failures than that of tunnels buried in either partially saturated soil or dry soil when subjected to the same surface explosion.

− In all soil types, the diametric distortions increase with the explosive mass and the distortions are irreversible in all load cases.

− The analytical curves developed in this study enable a quick and simple assessment of the vulnerability of buried tunnels subjected to surface blasts. A comparison of critical lines for identical scale distances illustrates that the tunnel lining is more vulnerable to surface explosions that occur directly above the centre of the tunnel than those that occur in the ground at any equivalent distance from the tunnel centre.

REFERENCES

[1] Jiang Q, Feng XT, Chen J, Huang K, Jiang YL. Estimating in-situ rock stress fromspalling veins: a case study. Eng Geol. 2013;152(1):38–47.

[2] Cai M, Kaiser PK. In-situ rock spalling strength near excavation boundaries. Rock Mech Rock Eng. 2014;47(2):659–675.

[3] Shemyakin EI, Fisenko GL, Kurlenya MV, et al. Zonal disintegration of rocks around underground workings, Part 1: data of in situ observations. Sov Min 1986;22(3):157–168.

[4] Jia P, Zhu WC. Mechanism of zonal disintegration around deep underground excavations under triaxial stress Insight from numerical test. Tunn Undergr Space Technol. 2015;48(11):1–10.

[5] Ortlepp WD, Stacey TR. Rockburst mechanisms in tunnels and shafts. Tunn Undergr Space Technol. 1994;9(1):59–65.

[6] Li SJ, Feng XT, Li ZH, Chen BR, Zhang CQ, Zhou H. In situ monitoring of rockburst nucleation and evolution in the deeply buried tunnels of Jinping II hydropower station. Eng Geol. 2012;137−138(7):85–96.

[7] Cai M. Influence of stress path on tunnel excavation response – Numerical tool selection and modeling strategy. Tunn Undergr Space Technol. 2008;23(6):618–628.

[8] Lu WB, Yang JH, Yan P, et al. Dynamic response of rock mass induced by the transient release of in-situ stress. Int J Rock Mech Min Sci. 2012;53(9):129–141.

[9] Yang JH, Yao C, Jiang QH, Lu WB, Jiang SH. 2D numerical analysis of rock damage induced by dynamic in-situ stress redistribution and blast loading in underground blasting excavation. Tunn Undergr Space Technol. 2017;70:221–232.

[10] Fan Y, Lu WB, Yan P, Chen M, Zhang YZ. Transient characters of energy changes induced by blasting excavation of deep-buried tunnels. Tunn Undergr Space Technol. 2015;49:9–17.

[11] Weng L, Huang LQ, Taheri A, Li XB. Rockburst characteristics and numerical simulation based on a strain energy density index: a case study of a roadway in Linglong gold mine, China. Tunn Undergr Space Technol. 2017;69:223–232.

[12] Germanovich LN, Dyskin AV. Fracture mechanisms and instability of openings in compression. Int J Rock Mech Min Sci. 2000;37(1):263–284.

[13] Martino JB, Chandler NA. Excavation-induced damage studies at the Underground Research Laboratory. Int J Rock Mech Min Sci. 2004;41(8):1413–1426.

[14] Read RS. 20 years of excavation response studies at AECL's Underground Research Laboratory. Int J Rock Mech Min Sci. 2004;41(8):1251–1275.

[15] Golshani A, Oda M, Okui Y, Takemura T, Munkhtogoo E. Numerical simulation of the excavation damaged zone around an opening in brittle rock. Int J Rock Mech Min Sci. 2007;44(6):835–845.

[16] Zhu WC, Bruhns OT. Simulating excavation damaged zone around a circular opening under hydromechanical conditions. Int J Rock Mech Min Sci. 2008;45(5):815–830.

[17] Wang HW, Jiang YD, Xue S, et al. Assessment of excavation damaged zone around roadways under dynamic pressure induced by an active mining process. Int J Rock Mech Min Sci. 2015;77:265–277.

[18] Shin JH, Moon HG, Chae SE. Effect of blast-induced vibration on existing tunnels in soft rocks. Tunn Undergr Space Technol. 2011;26(1):51–61.

[19] Liang QG, Li J, Li DW, Ou E. Effect of blast-induced vibration from new railway tunnel on existing adjacent railway tunnel in xinjiang. China Rock Mech Rock Eng. 2013;46(1):19–39.

[20] Yu HT, Yuan Y, Yu GX, Liu X. Evaluation of influence of vibrations generated by blasting construction on an existing tunnel in soft soils. Tunn Undergr Space Technol. 2014;43(7):59–66.

[21] Ainalis D, Kaufmann O, Tshibangu JP, Verlinden O, Kouroussis G. Modelling the source of blasting for the numerical simulation of blast-induced ground vibrations: a review. Rock Mech Rock Eng. 2017;50(1):171–193.

[22] Hao H, Wu C, Seah CC. Numerical analysis of blast-induced stress waves in a rock mass with anisotropic continuum damage models part 2: stochastic approach. Rock Mech Rock Eng. 2002;35(2):95–108.

[23] Wu CQ, Lu Y, Hao H. Numerical prediction of blast-induced stress wave from largescale underground explosion. Int J Numer Anal Methods Geomech. 2004;28(1):93–109.

[24] Malmgren L, Nordlund E. Behaviour of shotcrete supported rock wedges subjected to blast-induced vibrations. Int J Rock Mech Min Sci. 2006;43(4):593–615.

[25] Dhakal RP, Pan TC. Response characteristics of structures subjected to blasting-induced ground motion. Int J Impact Eng. 2003;28(8):813–828.

[26] Chen HL, Xia ZC, Zhou JN, Fan HL, Jin FN. Dynamic responses of underground arch structures subjected to conventional blast loads: curvature effects. Arch Civ Mech Eng. 2013;13(3):322–333.

[27] Mitelman A, Elmo D. Analysis of tunnel support design to withstand spalling induced by blasting. Tunn Undergr Space Technol. 2016;51:354–361.

[28] Jing L, Hudson JA. Numerical methods in rock mechanics. Int J Rock Mech Min Sci. 2002;39(4):409–427.

[29] Jing L. A review of techniques, advances and outstanding issues in numerical modelling for rock mechanics and rock engineering. Int J Rock Mech Min Sci. 2003;40(3):283–353.

[30] Stamos AA, Beskos DE. Dynamic analysis of large 3-D underground structures by the BEM. Earthq Eng Struct D. 1995;24(6):917–934.

[31] Wang ZL, Li YC, Shen RF. Numerical simulation of tensile damage and blast crater in brittle rock due to underground explosion. Int J Rock Mech Min Sci. 2007;44(5):730–738.

[32] Ning YJ, Yang J, An XM, Ma GW. Modelling rock fracturing and blast-induced rock mass failure via advanced discretisation within the discontinuous deformation analysis framework. Comput Geotechnol.2011;38(1):40-49.

[33] Ning YJ, Yang J, Ma GW, Chen PW. Modelling rock blasting considering explosion gas penetration using discontinuous deformation analysis. Rock Mech Rock Eng. 2011;44(4):483–490

[34] Jayasinghe LB, Thambiratnam D, Perera NJ, Jayasooriya R. Effect of soil properties on the response of pile to underground explosion. Struct. Eng. Int. 2014; 24(3): 361–370.

[35] Wen D, Poh J, Ng YW. Design considerations for bored tunnels at close proximity. Tunn. Undergr. Space Tech. 2004; 19(4–5): 468–469.